JOURNAL OF MATERIALS SCIENCE **38** (2003) 1667–1672

Corrosion fatigue of austempered ductile iron

CHIH-KUANG LIN*, CHANG-HAO YANG, JENG-HO WANG
Department of Mechanical Engineering, National Central University, Chung-Li 32054, Taiwan
E-mail: t330014@cc.ncu.edu.tw

Corrosion fatigue (CF) behavior has been investigated for an austempered ductile iron (ADI) by conducting systematic fatigue tests at 20 Hz, including both high-cycle fatigue (HCF, S-N curves) and fatigue crack growth (FCG, da/dN-ΔK curves), in air, lubrication oil and several aqueous environments. Results showed the HCF resistance of ADI was dramatically reduced by the given aqueous media, in particular, to a greater extent with a decrease in pH value. However, the given room-temperature aqueous solutions did not exert significantly detrimental effects on the Stage II crack growth compared with an atmospheric environment but an increase in solution temperature caused enhanced Stage II crack growth. Among the given variables of the bulk environment, pH had the greatest influence on HCF response while temperature had the most influence on the FCG of long cracks. In addition, SAE 10W40 lubrication oil provided an inert environment to remove the corrosive effect and enhance the CF resistance of ADI. The overall comparisons indicated the environmental effects would generate more influence on Stage I cracking than on Stage II cracking for the given ADI.

1. Introduction

Austempered ductile irons (ADIs) offer excellent combinations of high tensile strength, ductility, toughness, fatigue strength and wear resistance compared with other grades of cast irons [1–3]. These desirable mechanical properties are comparable, or in some cases superior to those of forged steel as a result of an unique ausferrite matrix structure consisting of acicular, carbide-free ferrite with carbon-enriched austenite. Low density and low cost in near-net-shape forming of complex geometries are additional advantages of ADIs over forgings. Therefore, ADI is an attractive material for many engineering applications in heavy machinery, transportation equipment and other industries [1–3]. As the use of ADI castings in many applications involves long-term, mechanical variable loads under corrosive environments, it is important to understand the corrosion fatigue (CF) behavior of this advanced cast iron for design and life assessment purposes.

Previous studies in fatigue properties of ADI were mainly focused on atmospheric environments including, e.g., high-cycle fatigue (HCF) [4–11], strain-controlled low-cycle fatigue (LCF) [12–15], and fatigue crack growth (FCG) [16–20]. The fatigue limit of ADI in HCF is not proportional to tensile strength but increases with both the retained austenite content and the carbon content of the retained austenite [1, 4–11]. However, Lin *et al.* [10–13] found that ADI having a larger volume fraction of retained austenite showed better HCF strength but inferior LCF resistance. This is due to the stability of retained austenite under various fatigue loading modes [10–13]. With regard to FCG behavior in ADI, the fatigue crack growth rate (FCGR) was found to be lower in a coarse ausferritic matrix structure with a greater retained austenite content [6, 16, 17, 20] while one study [18] indicated it was rarely affected by the difference in the ausferritic matrix structures. However, very little work [21–23] has be done on the CF characteristics of ADI and the limited results and discussion were focused either on the HCF or FCG behavior only. Those results [21–23] therefore could not distinguish the environmental effect on the fatigue crack initiation and propagation stages separately, given a alloy composition and austempering treatment. As part of a series of studies [9–14, 20, 23] on the assessment of ADI fatigue behavior, the present work was therefore planned to characterize the environmental effects on the fatigue crack initiation and propagation stages in ADI by conducting systematic experiments, including both HCF (S-N curve) and FCG (da/dN-ΔK curve), in air, lubrication oil and several aqueous environments. Hopefully, the experimental CF data of the current study in conjunction with the previous results [9–14, 20, 23] will provide some insight into fatigue behavior of ADI in various environments for development of fatigue design methodology of ADI components.

2. Experimental procedures

The cast ductile iron was obtained as Y-blocks with a chemical composition (wt%): 3.53 C, 2.27 Si, 0.47 Ni, 0.43 Cu, 0.22 Mn, 0.17 Mo, 0.04 Mg, 0.026 P, 0.009 S, and balance of Fe. The graphite structure in selected casting portions has an average nodule diameter of 34 μm, a nodularity of ~90%, and a nodule

*Author to whom all correspondence should be addressed.

count of ~90 nodules/mm^2. Fatigue specimens were austenitized at 900°C for 1.5 h and then austempered at 360°C for 2 h, both in salt bath. The mechanical properties of this grade of ADI have an ultimate tensile strength of 1,036 MPa, a yield strength of 901 MPa, an elastic modulus of 167 GPa, an elongation of 1.64% (in 25 mm), a hardness value of 38 HRc, and an impact toughness of 143 J. X-ray diffraction analysis indicated the average volume fraction of retained austenite is 30.3% in this ADI.

Both HCF and FCG tests were carried out at room temperature in laboratory air (relative humidity = 70%), SAE 10W40 lubrication oil and three aqueous environments: (1) distilled water (pH = 7.6); (2) 3.5 wt% NaCl solution (pH = 7.3); (3) 50 ppm H_2SO_4 solution (pH = 3). In order to examine the environmental temperature effect on the CF of ADI, additional sets of HCF and FCG tests were conducted in 3.5 wt% NaCl solution (pH = 7.3) at 80°C. All CF tests were conducted under freely corroding conditions, i.e., no external potential was applied to the specimens. HCF tests were conducted as per ASTM E466 on axial smooth-surface specimens, with a cylindrical gage section of 6 mm in diameter and 18 mm in length, to determine the stress-life (S-N) curves. FCG experiments were performed in accordance with ASTM E647 on 6.35-mm-thick compact tension (CT) specimens to determine the da/dN-ΔK curves. Details of the specimen geometry and experimental set-up for such CF tests were described elsewhere [23, 24]. All fatigue tests were performed on a closed-loop, servohydraulic machine under a sinusoidal loading wave form with a load ratio of R (minimum load/maximum load) = 0.1 and a frequency of $f = 20$ Hz. The HCF tests were run to failure or to 2×10^6 cycles where specimen was considered to be a runout. All CT specimens were first fatigue precracked in laboratory air before testing in the corrosive environments. The crack length in the FCG test was determined by the compliance technique recommended by ASTM E647 using a clip gage mounted on the front edge of the CT specimen to monitor the crack-mouth-opening displacement during testing. Characterizations of the fracture surface morphology were made by scanning electron microscopy (SEM).

The corrosion potential and corrosion rate (corrosion current density) of the given ADI in various given solutions were obtained using a commercial potentioscan instrument by extrapolation of the anodic and cathodic Tafel slopes of the anodic and cathodic polarization curves at the linear Tafel region. Note that all potentials were measured with reference to a saturated calomel electrode (SCE) and platinum wires were used as the counter electrodes. The measured values of corrosion current density and corrosion potential for the given alloy/environment systems are present in Table I.

TABLE I Corrosion rates and corrosion potentials for ADI tested in various aqueous media

Environment	Corrosion current density (μA/cm^2)	Corrosion potential (mV$_{SCE}$)
Distilled water, RT, pH = 7.6	4.52	−640
50 ppm H_2SO_4, RT, pH = 3	30.2	−676
3.5% NaCl, RT, pH = 7.8	10.5	−672
3.5% NaCl, 80°C, pH = 7.6	22.6	−713

3. Results and discussion

3.1. Fatigue behavior in various environments at room temperature

The S-N curves for HCF specimens tested in lubrication oil, air and three aqueous media (distilled water, salt water and sulfuric acid solution) at room temperature are given in Fig. 1. The straight solid and dash lines in Fig. 1 represent the best-fit S-N curves by a linear regression analysis. Fig. 1 clearly demonstrates deleterious effects of the three aqueous environments on the HCF response of ADI, as a remarked reduction of fatigue life was found in each aqueous solution compared to atmospheric air. The counterpart results of the FCG tests using pre-cracked CT specimens in the corresponding environments were plotted as (da/dN) vs. (ΔK) in Fig. 2 where the FCGRs in air were not

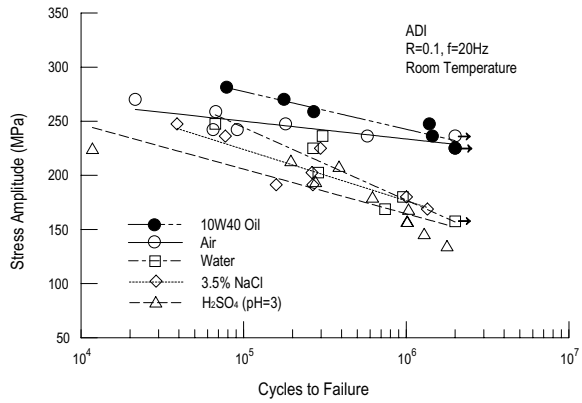

Figure 1 S-N curves for ADI tested at 20 Hz in various room-temperature environments. (Arrows designate runout tests.)

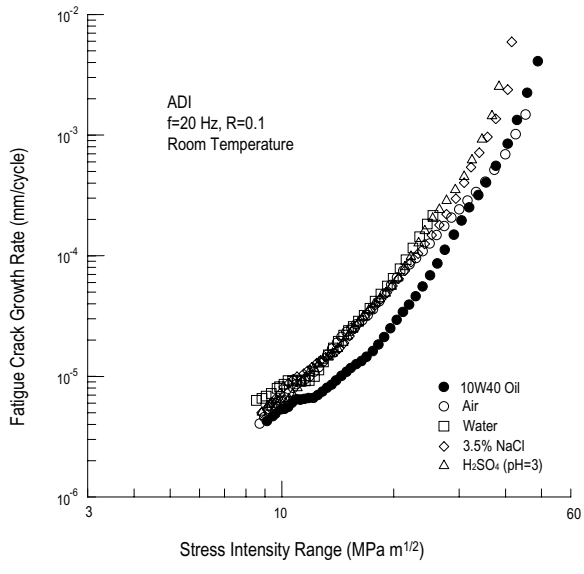

Figure 2 Fatigue crack growth rate curves for ADI tested at 20 Hz in various room-temperature environments.

significantly different from those in the aqueous environments except at the ΔK region near final fast fracture. Apparently, these aqueous media did not generate as severe damage on the FCG resistance of pre-cracked CT specimens (Stage II cracking only) as they did in the case of smooth-surface HCF specimens (including crack initiation, Stage I and Stage II cracking) under a cyclic load of 20 Hz.

It has been fully discussed in a previous study [23] that the lack of corrosive effect from the given aqueous media on the long fatigue crack growth at 20 Hz, as seen in Fig. 2, could be attributed to two reasons. Firstly, a similar CF damage mechanism such as hydrogen embrittlement (HE) were slightly operative in the given humid air and three aqueous solutions under 20 Hz cyclic loading, as the FCGRs in atmospheric air were somewhat higher than those in inert oil (Fig. 2) [23]. Secondly, a high frequency of fatigue loading such as 20 Hz did not provide enough time in each cycle for the surface reactions related to HE to fully function in the three given aqueous media [23]. This was evidenced by the fact that the FCGRs in the three given aqueous solutions were effectively enhanced from those in air as loading frequency was reduced from 20 to 1 Hz [23]. However, as shown in Fig. 1, fatigue loading at 20 Hz combined with the three given aqueous media did generate considerably adverse effects to reduce the HCF lives from the air values. Fig. 1 also shows the HCF lifetime was extended in an lubrication oil compared to the atmospheric air indicating the humid air, relative to the inert oil, was more or less a corrosive environment to the HCF resistance of ADI. These overall comparisons between HCF and FCG results indicated the HCF life was controlled by the crack nucleation stage and the corrosive effect on the CF resistance of ADI was mainly exerted on the phase of crack initiation and Stage I crack growth rather than on the phase of Stage II crack growth. Similar conclusions have been drawn for steels [25, 26] that the fatigue lifetime in aggressive environments was controlled by early growth of initial defects or short cracks of microstructural dimensions. Although several CF processes may occur throughout the lifetime, the governing mechanisms are those that strongly depend on the synergism between cyclic stresses and aggressive environment which often leads to strain localization and enhanced growth of defects and short cracks [25]. These controlling processes include pitting, preferential dissolution, Stage I crack growth and transition from Stage I-to-Stage II crack growth [25]. It is generally recognized that corrosion pits and/or localized corrosion of emerging slip steps or extrusions, somehow induced by CF processes, prematurely initiate fatigue cracking or reduce the applied stress required to initiate fatigue cracks [25, 27, 28].

The time required to form a fatigue crack nucleus in ductile iron is essentially short [29], and, for ADI, fatigue crack initiation generally occurs at graphite nodules (due to weak nodule/matrix interface bond) and casting imperfections (due to severe stress concentration) including microshrinkage pores, inclusions and irregularly shaped graphite clusters [10, 11]. SEM fractography observations revealed that in the current study fatigue cracks mostly initiated at surface or subsurface microshrinkage pores in all given environments and no visible corrosion pits were detected around fracture origins in any of the given aqueous solutions, as exemplified by Figs 3 and 4. In other words, the fatigue fracture origins for the given ADI in lubrication oil, air and various aqueous solutions are of no significant difference and commonly located at microshrinkage pores due to severe stress concentration. Apparently, fatigue cracks initiated more easily at the microshrinkage pores than at any corrosion-induced surface defects (such as pits) for the given material/environment systems. Therefore, the significant reduction of HCF life in ADI by the three given aqueous solutions could be attributed to the enhanced growth of short fatigue crack nuclei (such as microshrinkage pores and large debonded nodule voids) and reduced length of transition period from Stage I to Stage II crack growth. In particular, the enhanced growth of fatigue crack nuclei in the given aqueous environments was likely assisted by the mechanisms such as preferential dissolution and/or HE with the absence of corrosion pitting.

Ausferrite packet boundaries and prior austenite grain boundaries are recognized as the microstructural barriers to short fatigue crack nuclei in ADI and play an important role in determining the fatigue strength [19]. With the assistance of a corrosive environment, the short fatigue crack nuclei could cross these microstructural barriers with less difficulty leading to a

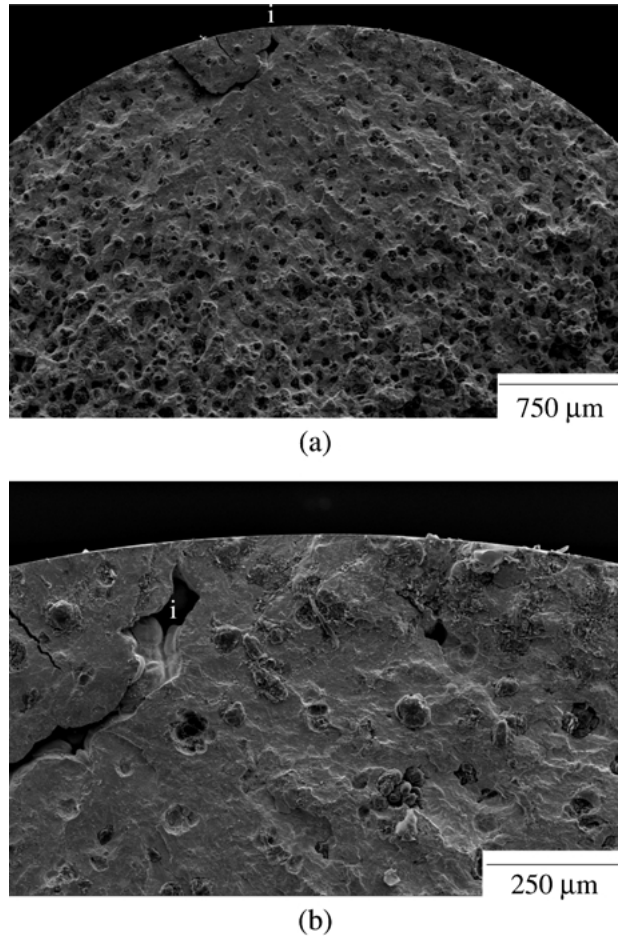

Figure 3 SEM fractography of an ADI HCF specimen tested in air: (a) slow crack growth region and (b) fracture origin. (i: crack initiation site.)

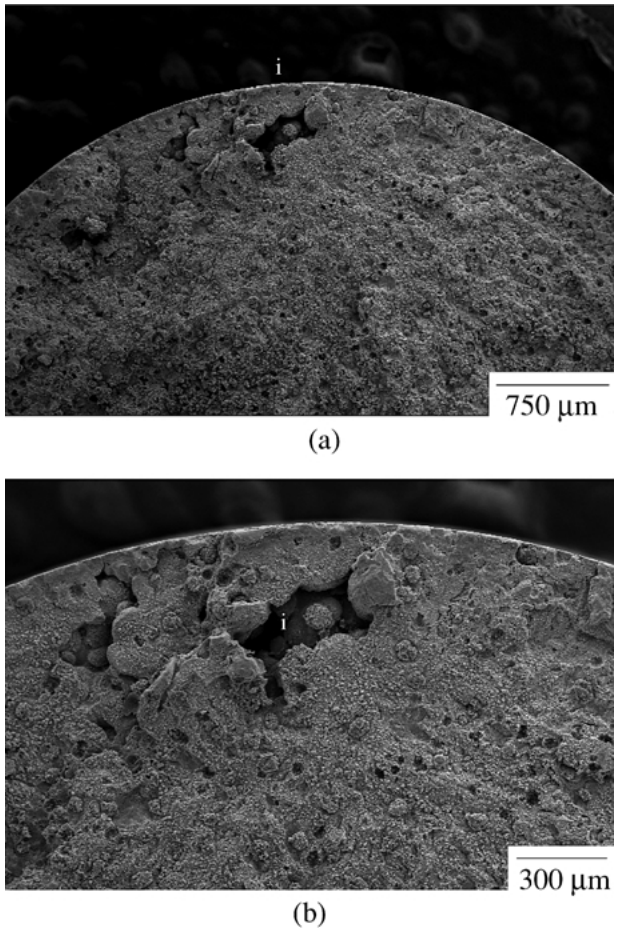

Figure 4 SEM fractography of an ADI HCF specimen tested in 3.5% NaCl: (a) slow crack growth region and (b) fracture origin. (i: crack initiation site.)

shorter fatigue life. The severity of the environmental effect on the HCF resistance of ADI is related to the nature of the corrosive environment. Among the three given aqueous solutions, sulfuric acid solution is the most aggressive in reducing the HCF resistance, followed by the salt water and then the distilled water. This is consistent with the electrochemical data presented in Table I, where ADI has the highest corrosion rate (corrosion current density) in sulfuric acid solution. As no clear passive range can be defined in the electrochemical polarization curves, the metal-dissolution behavior for the given ADI in the given three room-temperature aqueous solutions is likely to be active corrosion or general corrosion over pitting corrosion. This is also evidenced by the fractography observation that no visible corrosion pits were found on the HCF specimens even in the salt water where the well-known pit-provoking ion, chloride, was present. The higher corrosion rate of ADI in sulfuric acid solution over neutral salt water and distilled water can be attributed to an increase in the hydrogen ion concentration and then an increase in metal dissolution in an acid solution. In this regard, the controlling CF mechanisms such as preferential dissolution at slip bands and HE at crack tip in an acid medium would be more active in assisting the surface and subsurface fatigue crack nuclei of ADI to overcome the microstructural barriers and accelerate the initial growth. As a result, ADI shows the greatest reduction of HCF lifetime in sulfuric acid solution compared to neutral salt water and distilled water. Table I also shows, due to the presence of chloride, salt water is more aggressive than distilled water which explains why the HCF life is shorter in salt water than in distilled water.

Apparently, the crack initiating processes in ADI are more vulnerable to the variation of bulk environment characteristics than the processes associated with Stage II cracking, as the HCF life varied distinctly with the nature of bulk environment but the FCGRs of long cracks were comparable in the given environments (except lubrication oil) under a fatigue load of 20 Hz. An earlier study [23] has shown that for the same given material/environment system at 1 Hz, the FCGRs of long cracks in aqueous environments were considerably greater than those in air but still comparable with each other regardless of the class of ion species and pH in the bulk solution. The insensitivity of the FCGR of a long crack to the ion species and pH in bulk solution was likely due to a similar acid aqueous environment at the crack tip region as a result of a local acidification process involving dissolution of Fe and subsequent hydrolysis of Fe^{+2} in the occluded solution within the crack tip [23, 30, 31]. Therefore, the bulk aqueous solutions might be different but the local crack tip environments responsible for long crack growth were comparable and produced equivalent FCGRs at the given loading frequency. However, this type of acidification process might hardly be active within the surface/subsurface short fatigue cracks for ADI because the HCF life, controlled by the nucleation and growth of short fatigue cracks, was indeed a function of the ion species and pH in bulk solution.

3.2. Effect of environmental temperature on the corrosion fatigue behavior

The influence of environmental temperature on CF behavior of ADI was investigated by conducting additional sets of HCF and FCG tests in 3.5 wt% NaCl solution at 80°C. The S-N curves for the given ADI tested in neutral salt water at room temperature and 80°C are plotted for comparison in Fig. 5. With the consideration of data scattering in Fig. 5, the temperature effect on the

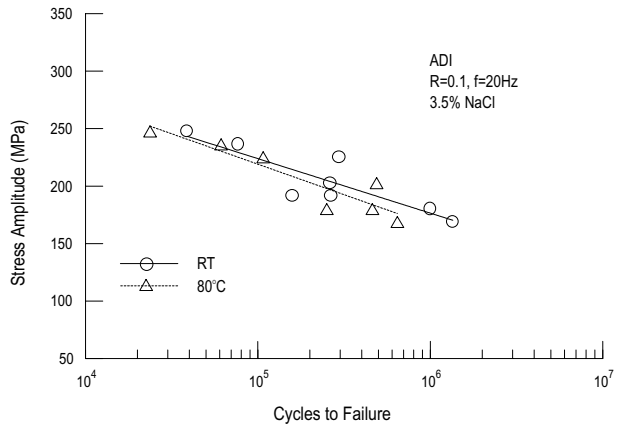

Figure 5 Comparison of S-N curves for ADI tested in 3.5% NaCl solutions at different temperatures.

HCF response is considered to be small, although the best-fit curve for the room temperature data is slightly higher than the 80°C one. Comparisons of the corresponding FCGR data for a long crack are shown in Fig. 6 where a clear enhancement of FCGR could be seen for increasing salt water temperature from room temperature to 80°C. The aqueous solution at 80°C presumably provided higher activation energy for the CF mechanisms controlling fatigue crack nucleation and propagation to proceed and accelerate crack development, compared to the room temperature solution. In other words, the influence of environmental temperature on the CF response is reflected through its effect on the rate of electrochemical reactions at the metal-water interface and/or hydrogen diffusion at the crack tip region. As both the reactions- and diffusion-controlled mechanisms are temperature dependent by the Arrhenius law [32], the growth of both short and long fatigue cracks is expected to increase with increasing temperature, as evidenced in Figs 5 and 6. The electrochemical data in Table I consistently indicate that an increase in temperature of the neutral salt water increased the corrosion rate, presumably, due to the increased kinetics of metal dissolution. However, the change of salt water temperature from room temperature to 80°C apparently exerted more influence on HE at crack tip than on preferential dissolution at slip bands, as a greater temperature effect on the FCG response (Fig. 6) than on the HCF response (Fig. 5) was observed. These observations clearly demonstrate that the CF of ADI in an aqueous environment is a thermally activated process and its environmental temperature dependence is reflected through the influence of temperature on the rate controlling processes in preferential dissolution and HE mechanisms. In addition, comparison of Figs 2 and 6 indicate that under a fatigue load of 20 Hz, temperature is more effective in enhancing the FCGR of long cracks in ADI than the other bulk solution variables such as pH and ion species, as the local crack-tip conditions for a given temperature might be similar for different bulk aqueous solutions due to the local acidification process described above.

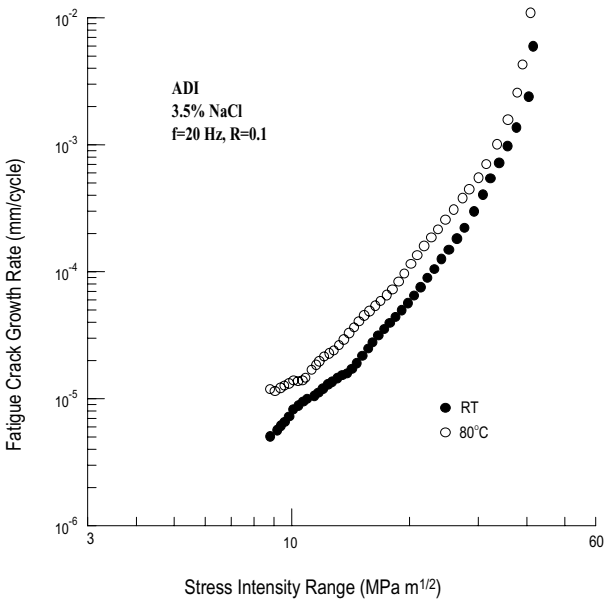

Figure 6 Comparison of fatigue crack growth rate curves for ADI tested in 3.5% NaCl solutions at different temperatures.

4. Conclusions

1. The HCF life in ADI was controlled by the early growth of fatigue crack nuclei which was more sensitive to the environmental effect than the Stage II crack growth, as the HCF lifetimes of smooth specimens were shorter in three given aqueous media than in atmospheric air while the corresponding FCGRs of long cracks were not significantly different.

2. Sulfuric acid solution was more aggressive than neutral salt water and distilled water in reducing the HCF life of ADI due to a higher corrosion rate in metal dissolution which more effectively enhanced the growth of short fatigue crack nuclei.

3. SAE 10W40 oil could provide an inert environment for ADI to decrease the FCGR and extend the HCF life in comparison to atmospheric air and aqueous solutions.

4. The CF mechanisms in ADI were influenced by certain thermally activated processes as the fatigue resistance, in particular for a long crack, of ADI in salt water was decreased with an increase in environmental temperature from room temperature to 80°C.

Acknowledgements

This work was funded by the National Science Council of the Republic of China (Taiwan) under Contract No. NSC-89-2216-E-008-005.

References

1. Y. TANAKA and H. KAGE, *Mater. Trans., JIM* **33** (1992) 543.
2. B. V. KOVACS, *J. Heat Treat.* **5** (1987) 55.
3. T. N. ROUNS, K. B. RUNDMAN and D. M. MOORE, *AFS Trans.* **92** (1984) 815.
4. M. GRECH and J. M. YOUNG, *ibid.* **98** (1990) 341.
5. K. P. JEN, J. WU and S. KIM, *ibid.* **100** (1992) 833.
6. L. BARTOSIEWICZ, A. R. KRAUSE, F. A. ALBERTS, I. SINGH and S. K. PUTATUNDA, *Materials Characterization* **30** (1993) 221.
7. P. SHANMUGAN, P. P. RAO, K. R. UDUDA and N. VENKATARAMAN, *J. Mater. Sci.* **29** (1994) 4933.
8. M. BAHMANI, R. ELLIOTT and N. VARAHRAM, *ibid.* **32** (1997) 5383.
9. C.-K. LIN and W.-J. LEE, *Int. J. Fatigue* **20** (1998) 301.
10. C.-K. LIN, P.-K. LAI and T.-S. SHIH, *ibid.* **18** (1996) 297.
11. C.-K. LIN and J.-Y. WEI, *Mater. Trans., JIM* **38** (1997) 682.
12. C.-K. LIN and T.-P. HUNG, *Int. J. Fatigue* **18** (1996) 309.
13. C.-K. LIN and C.-S. FU, *Mater. Trans., JIM* **38** (1997) 693.
14. C.-K. LIN and Y.-L. PAI, *Int. J. Fatigue* **21** (1999) 45.
15. J.-R. HWANG, C.-C. PERNG and Y.-S. SHAN, *ibid.* **12** (1990) 481.
16. J.-L. DOONG and S.-I. YU, *ibid.* **10** (1988) 219.
17. L. BARTOSIEWICZ, A. R. KRAUSE, B. KOVACS and S. K. PUTATUNDA, *AFS Trans.* **100** (1992) 135.
18. G. L. GRENO, J. L. OTEGUI and R. E. BOERI, *Int. J. Fatigue* **21** (1999) 35.
19. T. J. MARROW and H. CETINEL, *Fatigue Fract. Eng. Mater. Struct.* **23** (2000) 425.
20. C.-K. LIN and C.-W. CHANG, *J. Mater. Sci.* **37** (2002) 709.
21. S. MUTHUKUMARASAMY and S. SESHAN, *AFS Trans.* **100** (1992) 873.
22. M. N. JAMES and W. LI, *Mater. Sci. Eng.* A **265** (1999) 129.

23. C.-K. LIN and J.-H. WANG, *Mater. Trans., JIM* **42** (2001) 1085.
24. C.-K. LIN and S.-T. YANG, *Eng. Fract. Mech.* **59** (1998) 779.
25. K. J. MILLER and R. AKID, *Proc. R. Soc. Lond.* A **452** (1996) 1411.
26. C.-K. LIN and W.-J. TSAI, *Fatigue Fract. Eng. Mater. Struct.* **23** (2000) 489.
27. C. LAIRD and D. J. DUQUETTE, in "Corrosion Fatigue: Chemistry, Mechanics and Microstructure," edited by O. Devereux, A. J. McEvily and R. W. Staehle (National Association of Corrosion Engineers, Houston, USA, 1972) p. 88.
28. D. J. MCADAM, *Proc. ASTM* **26** (1926) 224.
29. D. F. SOCIE and J. FASH, *AFS Trans.* **90** (1982) 385.
30. B. F. BROWN, C. T. FUJII and E. P. DAHLBERG, *J. Electrochem. Soc.* **116** (1969) 218.
31. G. SANDOZ, C. T. FUJII and B. F. BROWN, *Corrosion Sci.* **10** (1970) 839.
32. R. P. WEI and M. GAO in "Hydrogen Effects on Mechanical Behavior," edited by N. R. Moody and A. W. Thompson (The Minerals, Metal and Materials Society, Warrendale, PA, USA, 1990) p. 789.

Received 1 July
and accepted 24 December 2002